The clustering and morphology of chondrocytes in normal and mildly degenerate human femoral head cartilage studied by confocal laser scanning microscopy

The clustering and morphology of chondrocytes in normal and mildly degenerate human femoral head cartilage studied by confocal laser scanning microscopy.

Asima Karim[1#], Anish K. Amin[2] and Andrew C. Hall[1]*

[1]Centre for Integrative Physiology, Deanery of Biomedical Sciences, University of Edinburgh, Edinburgh, U.K.

[2]Department of Orthopaedic and Trauma Surgery, University of Edinburgh, Edinburgh, U.K.

*Address for correspondence
Dr. Andrew C. Hall,
Centre for Integrative Physiology,
Deanery of Biomedical Sciences,
Hugh Robson Building,
George Square,
Edinburgh EH8 9XD,
Scotland, United Kingdom.
E.mail: a.hall@ed.ac.uk
Phone +44 (0)131 650 3263
FAX: (+44) (0)131 650 2872

[#]Present address:
Department of Physiology & Cell Biology
University of Health Sciences, Lahore.
E.mail: akarim@exseed.ed.ac.uk
Phone: 92-042-99231304 / 09 Ext.334

Running title: *Chondrocytes in human cartilage*

Key words: chondrocyte morphology; chondrocyte clustering; cytoplasmic processes; femoral head; cartilage; confocal laser scanning microscopy.

Total number of text figures and tables: 6 figures & 0 tables.

ABSTRACT

Chondrocytes are the major cell type present in hyaline cartilage and they play a crucial role in maintaining the mechanical resilience of the tissue through a balance of the synthesis and breakdown of extracellular matrix macromolecules. Histological assessment of cartilage suggests that articular chondrocytes *in situ* typically occur singly and demonstrate a rounded/elliptical morphology. However there are suggestions that their grouping and fine shape is more complex and that this changes with cartilage degeneration as occurs in osteoarthritis. In the present study we have used confocal laser scanning microscopy and fluorescently-labelled *in situ* human chondrocytes and advanced imaging software to visualise chondrocyte clustering and detailed morphology within grade-0 (non-degenerate) and grade-1 (mildly-degenerate) cartilage from human femoral heads. Graded human cartilage explants were incubated with 5-chloromethylfluorescein diacetate and propidium iodide to identify the morphology and viability respectively of *in situ* chondrocytes within superficial, mid and deep zones. In grade-0 cartilage, the analysis of confocal microscope images showed that while the majority of chondrocytes were single and morphologically normal, clusters (i.e. ≥3 chondrocytes within the enclosed lacunar space) were occasionally observed in the superficial zone, and 15-25% of the cell population exhibited at least one cytoplasmic process of ~5μm in length. With degeneration, cluster number increased (~50%) but not significantly, however the number of cells/cluster (P<0.001) and the percentage of cells forming clusters increased (P=0.0013). In the superficial zone but not the mid- or deep zones, the volume of clusters and average volume of chondrocytes in clusters increased (P<0.001; P<0.05 respectively). The percentage of chondrocytes with processes, the number of processes/cell and the length of processes/cell increased in the superficial zone of grade-1 cartilage (P=0.0098; P=0.02; P<0.001 respectively). Processes were categorised based on length (L0 – no cytoplasmic processes; L1<5μm; 5<L2≤10μm; 10<L3≤15μm; L4>15μm). With cartilage degeneration, for chondrocytes in all zones, there was a significant decrease (P=0.015) in the percentage of chondrocytes with

59 'normal' morphology (i.e. L0), with no change in the percentage of cells with L1 processes,
60 however there were significant increases in the other categories. In grade-0 cartilage, chondrocyte
61 clustering and morphological abnormalities occurred and with degeneration these were exacerbated,
62 particularly in the superficial zone. Chondrocyte clustering and abnormal morphology are
63 associated with aberrant matrix metabolism suggesting that these early changes to chondrocyte
64 properties may be associated with cartilage degeneration.
65

INTRODUCTION

Articular cartilage has a highly-specialised structure which imparts remarkable load-bearing properties over many decades. Chondrocytes are the major cell type and primarily responsible for the maintenance of the resilient extracellular matrix, and a small but distinct population of cartilage-derived stem/progenitor cells has also been reported (Dowthwaite et al., 2004). Cartilage properties vary with depth from the superficial zone, through to the mid-zone and finally the deep zone. These zones and their resident chondrocytes have different biomechanical (Chen et al. 2001; Vanderploeg et al. 2008) and metabolic properties (Aydelotte & Kuettner, 1988; Wong et al. 1996; Simpkin et al. 2007). From histological studies, the topographical arrangement and morphology of chondrocytes within the zones of normal (non-degenerate) articular cartilage have been described (Hunziker, 1992). While there are differences between animal species and joints, in non-degenerate cartilage, cell shape and distribution vary with depth. Superficial zone chondrocytes tend to have an elliptical, flattened appearance lying parallel to the surface. Mid-zone chondrocytes are spheroidal and randomly arranged whereas deep zone chondrocytes are almost all rounded and aligned in perpendicular columns. These adaptations are probably related to the prevailing biomechanical forces, which range from predominantly shearing/tensional stresses in the superficial zone, to mainly compressional forces in the deep zone (Grodzinsky et al. 2000). Chondrocyte clustering is also a property of some normal cartilages. For example, in the superficial zone of human ankle cartilage, horizontal cell clustering (described as 'strings') parallel to the surface occurs (Schumacher et al. 2002; Rolauffs et al. 2010). However clustering is more usually associated with degenerative joint disease (also known as osteoarthritis) where increased cell number and size are often localised near surface fissures (Lotz et al. 2010). Associated with cartilage degeneration, there are substantial changes to the cells and matrix, leading to a loss in zonal characteristics (Buckwalter & Mankin, 1997) and increased chondrocyte proliferation (Rothwell & Bentley, 1973; Rolauffs al. 2010; Lotz et al. 2010) possibly resulting from changes to the chondron microenvironment (Poole et al. 1991).

There is increasing evidence that human chondrocyte morphology is, however, more varied than these 'classical' elliptical/spheroidal forms (Bush & Hall, 2003; Murray et al. 2010). Advances have been made in the visualisation of living *in situ* chondrocyte morphology using fluorescent dyes and confocal scanning laser microscopy (Bush & Hall, 2003). Approximately half of the chondrocytes within macroscopically normal (non-degenerate, aged) human tibial plateau cartilage, have cytoplasmic processes extending beyond the pericellular matrix/lacuna into the inter-territorial matrix (Bush & Hall, 2003). Similar abnormal 'fibroblastic-like' chondrocytes have been observed in human femoral head cartilage overlaid with pannus (Holloway et al. 2004) and in histological/electron microscopical studies of normal and fibrillated human knee cartilage (Kouri et al. 1998; Tesche & Miosge, 2005). The processes are not related to the chondrocyte primary cilium (McGlashen et al. 2008).

The development of abnormal chondrocyte morphology in non-degenerate cartilage could be important as there is a close relationship between the actin cytoskeleton, a major controller of chondrocyte morphology (Blaine, 2009) and chondrocyte differentiation (Mallein-Gerin et al. 1991; Rottmar et al. 2014). Chondrocytes are phenotypically unstable and cytoskeletal integrity can affect matrix metabolism and thus potentially, cartilage resilience. For example, during chondrocyte de-differentiation, expression of cartilage markers of the transcription factor SOX9, and production of cartilage-specific matrix molecules (aggrecan, collagen Type II) are reduced, whereas synthesis of fibro-cartilageneous constituents (e.g. Type I collagen) is increased (Stokes et al. 2001; Woods et al. 2007). However, de-differentiation is reversible as chondrocytes with 'fibroblastic' morphology re-express the chondrogenic phenotype upon restoration of a spheroidal shape e.g. in agarose culture (Benya & Shaffer, 1982) or with cytoskeletal disruption (Blaine, 2009).

To determine if there is a relationship between changes to chondrocyte clustering and morphology from classical (elliptical/spheroidal) forms to abnormal shapes/clusters and the degree of cartilage degeneration, we have classified clusters and morphology of *in situ* chondrocytes using a quantitative approach. We have obtained osteochondral explants from normal (non-degenerate;

grade-0) and mildly-degenerate (grade-1) human femoral head cartilage and then incubated them with 5-chloromethylfluorescein diacetate a cytoplasmic dye which fluoresces green within chondrocytes, and propidium iodide which fluoresces red and identifies dead chondrocytes. Using confocal scanning laser microscopy and imaging of relatively unperturbed *in situ* chondrocytes in standardised regions of interest in the superficial, mid- and deep zones of grade-0 and grade-1 cartilage, we have then determined (a) the average number of clusters, (b) the average number of cells per cluster, (c) the percentage of cells present in clusters, (d) the average volume of clusters (in μm^3) and (e) the average volume of individual cells in a cluster (in μm^3). For chondrocyte morphology, we have measured (a) the percentage of cells with cytoplasmic processes, (b) the number of processes per cell and (c) the average length of cytoplasmic processes (in μm). The results revealed the marked heterogeneity of human chondrocyte grouping and morphology particularly within normal (non-degenerate) cartilage where small chondrocyte clusters and short cytoplasmic processes were identified. Furthermore, there were marked changes to chondrocyte clusters and morphology with progression of cartilage degeneration from grade-0 (non-degenerate) to grade-1 (mildly-degenerate).

MATERIALS AND METHODS

Human femoral head articular cartilage.

Femoral heads were obtained with Ethical Permission (Tissue Governance, National Health Service, Lothian) from eleven patients (eight females, three males, 77.8±5.8yrs, (mean ± confidence intervals (95%); range 65-89yrs); grade-0 78.9±7.8yrs, range 64-89yrs; grade-1 76.6±9.2yrs, range 65-89yrs), undergoing surgery only for hip hemiarthroplasty due to fractured neck of femur. Heads were immediately transferred to Dulbecco's Modified Eagle's Medium (pH7.4) supplemented with penicillin/streptomycin (100Units/ml and 100µg/ml respectively; Invitrogen, Paisley, United Kingdom). Throughout, care was taken to avoid tissue injury during handling (Huntley et al. 2005) or dehydration (Paterson et al. 2015) with experiments being performed within 10h of surgery.

Cartilage grading.

Cartilage was assessed by a clinician (AA) and a biomedical scientist (AK) using Osteoarthritis Research Society International (OARSI) criteria (Pritzker et al. 2006). Visually, grade-0 cartilage was smooth and shiny with no roughness/fibrillations, whereas grade-1 cartilage areas were discoloured and appeared rough with occasional superficial splitting. The surface roughness of explants was visualised by adjusting the brightness/contrast of the confocal laser scanning microscope images further assisting cartilage grading (Fig.1). For most of the femoral heads the cartilage was non-degenerate (grade-0) over >75% of the surface. However, in some femoral heads, there were relatively small areas (covering approx. 25%) of grade-1 cartilage present mostly at two locations around the fovea - parafoveal posterior and parafoveal inferior. Pannus (Shibakawa et al. 2003) was not observed on any joints.

Cartilage harvesting and fluorescent labelling.

Osteochondral explants comprising the full cartilage thickness with subchondral bone were harvested from graded areas. Explants were trimmed to ~5x5 mm using fresh scalpel blades to minimise chondrocyte death (Amin et al. 2008) and stored in Dulbecco's Modified Eagle's Medium. They were then incubated with 5-chloromethylfluorescein diacetate and propidium iodide

(12.5μM; 10μM respectively; 2h; 21°C) to label living (green) and dead (red) cells respectively (Amin et al. 2008). Explants were washed in phosphate buffered saline, fixed (formaldehyde 4%v/v; Fisher Scientific, Leicestershire, United Kingdom) and mounted for imaging.

Confocal laser scanning microscopy.

Fluorescently-labelled *in situ* chondrocytes were imaged using a Zeiss Axioskop LSM510 (Carl Zeiss, Welwyn Garden City, United Kingdom) (E_x=488nm; 543nm for 5-chloromethylfluorescein diacetate; propidium iodide respectively), (E_m=505-530nm and 650nm respectively). Cartilage appearance, chondrocyte viability, thickness and delineation of zones was initially evaluated at low power (x10 dry; numerical aperture=0.3). Chondrocyte morphology/clustering was determined at high power (x40; numerical aperture=0.8). Sequential *z* stack images in axial and coronal planes to 100μm for low, and 50μm for high power magnification with intervals of 5μm and 1μm respectively (frame size 1024x1024 pixels) were obtained (Amin et al. 2008).

Demarcation of cartilage zones.

Criteria (Hembree et al. 2007) were applied which depended on the morphology and orientation of chondrocytes visualised with low-power (x10) images. Superficial zone chondrocytes tended to be ellipsoidal with their long axis orientation parallel to the cartilage surface and comprised ~10% of the cartilage thickness. Mid-zone chondrocytes tended to be spheroidal, more randomly orientated, and comprised ~60% of the cartilage thickness. Deep zone chondrocytes were spheroidal, frequently in columns preferentially oriented perpendicular to the tidemark with subchondral bone, and comprised ~30% of the tissue thickness.

Morphological analysis of *in situ* chondrocytes.

Quantitative data regarding chondrocyte clusters and cytoplasmic processes were obtained by three-dimensional analysis of high power (x40) images utilising Volocity™ (Improvision, Coventry, United Kingdom) (Amin et al. 2008). Human chondrocytes occur singly, in pairs or clusters within a lacuna, with a cluster comprising ≥3 chondrocytes within the enclosed lacunar space (Rolauffs et al. 2010). The volume of clusters was measured using Volocity™ against calibrated fluorescent

beads (Fluoresbrite™, Polyscience, Warrington, United Kingdom) (Bush & Hall, 2001). The number of cells/cluster was counted manually however it was not possible to measure the volume of individual chondrocytes accurately because cells were frequently touching and identifying the membrane edge was unreliable. Average cell volume in a cluster was determined as: Cell volume in a cluster (μm^3) = (total volume of cluster (μm^3))/(total number of cells in cluster). The total number of chondrocytes within the region of interest (dimensions; *x*, *y*, *z* of 228, 228, 50µm respectively) was counted, and the percentage of cells forming clusters calculated as: % cells in a cluster =100 x (number of cells forming clusters/total number of cells) %.

Spheroidal/elliptical chondrocytes with no cytoplasmic processes were considered to have 'normal' morphology. The morphology of chondrocytes with ≥1 cytoplasmic process was described as being 'abnormal' although it should be noted that this term referred only to the shape of the cells and did not refer to any other physiological or pathological changes (Bush & Hall, 2003). The percentage of abnormal chondrocytes was calculated as: Abnormal chondrocytes (%) =100 × (number of abnormal cells) / (number of normal + abnormal cells) %. The length of cytoplasmic processes (in µm) was determined by tracing in three dimensions from their initiation at the cell body to their end. Cells with/without processes were further categorised into five groups based on their length (L): (L0 no processes present, L1<5µm, 5<L2≤10µm, 10<L3≤15µm and L4>15µm) permitting a more detailed quantitative comparison between cells in the different zones. The percentage of chondrocytes with cytoplasmic processes in category was calculated as: Chondrocytes in length category (L1-4) (%) =100 × (number of cells with specific length category (L1-4)) / total number of cells with processes) %. The number of cells was counted in the specified regions of interest and cell density calculated as; Cell density (number of cells/mm^3 x 10^3) = total no. of cells labelled with 5-chloromethylfluorescein diacetate and propidium iodide/volume of cartilage imaged (μm^3).

Data presentation and analysis.

Data were presented as mean ± confidence intervals (95%) for *[N(n)]* with *N* representing the number of cartilage samples and *n* the number of chondrocytes. Histograms and statistical tests were performed using GraphPad Prism 6 (GraphPad, California, USA). Student's t-tests were used to compare data between grade-0 and grade-1 cartilage. One-way Analysis of Variance with Tukey's *post-hoc* test were applied for comparison between and within groups. Significance was accepted when $P<0.05$. An asterisk (*) indicated a significant difference according to Student's t-tests and the hash symbol (#) indicated a significant difference by Analysis of Variance. Single, double and triple symbols indicated significance for $P<0.05$, 0.01 and 0.001 respectively, with actual values given where appropriate in text.

RESULTS

Thickness and zones of human femoral head cartilage. Full-depth grade-0 cartilage was 1554±66µm (*N*=6; range 1398µm-1648µm; mean ± confidence intervals). Thickness when measured at four different areas [parafoveal anterior, parafoveal posterior, parafoveal superior and parafoveal inferior], was not different between these areas ($P>0.05$) [parafoveal anterior (1519±253µm; *N*=3), parafoveal posterior (1559±403µm; *N*=2), parafoveal superior (1618±40µm; *N*=3) and parafoveal inferior (1305±41µm; *N*=3)]. Grade-0 cartilage surface was smooth and regular, however, grade-1 cartilage was clearly uneven (Fig.1(c) *vs* 1(d)). Grade-1 cartilage thickness measurements were difficult because of the irregular surface and cartilage-bone interface. However, the thickness of grade-1 cartilage was 1512±85µm (*N*=5; range 1335µm-1665µm), and similar to grade-0 cartilage.

The superfical, mid- and deep zones were defined as 10%, 60% and 30% respectively of the overall cartilage depth (Hembree et al 2007) corresponding to zones of approximate thicknesses; superficial zone, 155µm; mid-zone 155-932µm; deep zone 466µm respectively (Fig.1 grade-0). Coronal images of grade-0 and grade-1 cartilage showed differences in chondrocyte orientation/morphology between zones. In grade-0 cartilage, zones could be demarcated reasonably

accurately from the characteristic pattern of chondrocytes with depth. However, in grade-1 cartilage, chondrocyte arrangement was disturbed and zone identification unclear. In the superficial zone, clusters were infrequent in grade-0, but clearly identified in grade-1 cartilage (Fig.1(c) *vs* 1(d)). While these images illustrated important features of grade-0 and -1 cartilage, high power magnification was essential to visualise fine morphological features of chondrocytes in non-degenerate cartilage and any changes in grade-1 cartilage.

Overview of grade-0 and grade-1 human femoral head cartilage (axial views). Images taken distant from any cut edge (Fig.2(a-d)) represented chondrocyte morphology within relatively unperturbed cartilage. In grade-0 cartilage, chondrocytes were mostly spheroidal/elliptical with few hypo-cellular areas (Fig.2(a)). However in grade-1, heterogeneity of chondrocyte morphology and absence of cells were evident (Fig.2(b)). Few propidium iodide-labelled cells were observed in both grades (Fig.2) suggesting minimal chondrocyte death associated with cartilage preparation. In grade-0 cartilage, some cells had cytoplasmic processes (Fig.2(c)), however, in grade-1, many chondrocytes exhibited abnormal morphology/processes, and some clustering was evident (Fig.2(d)). In grade-0 cartilage, processes were short (≤5µm) and 64±4%;[$N(n)$=11(1178)] were curled within the lacunar space, with approx. 36±4% having straight processes. However in grade-1, processes were longer (>5µm) with 53±5% and 46±5%[$N(n)$=5(563)] curled and straight respectively suggesting that with cartilage degeneration, lacunae were disrupted and processes extended into the inter-territorial matrix (Fig.2(c) *vs* 2(d)). Cell density was not different between zones [superficial zone (27.8±1.5; 28.6±3.0cells/mm^3 x10^3), mid-zone (13.8±1.1; 13.6±2.0cells/mm^3 x10^3), and deep zone (11.9±1.0; 12.8±1.6cells/mm^3 x10^3)] for grade-0 and grade-1 respectively N=5 for each). However, clustering in grade-1 was extensive, potentially compensating for chondrocyte loss with degeneration.

Chondrocyte properties in grade-0 and grade-1 human articular cartilage (coronal views). High power (x40) images (Fig.3) showed increased heterogeneity of chondrocyte morphology in grade-1 compared to grade-0 cartilage. Although the majority of chondrocytes in grade-0 exhibited

normal morphology, cells with fine cytoplasmic processes were routinely observed. Clustering was infrequent, but when present, there were only few chondrocytes/cluster. However, in grade-1, many large clusters involving numerous chondrocytes/cluster were observed with many individual chondrocytes exhibiting cytoplasmic processes. These changes in grade-1 cartilage appeared greatest in the superficial zone, less marked in the mid-zone and least in the deep zone (Fig.3).

Chondrocyte cluster formation.

(a) Number of clusters, number of chondrocytes/cluster and percentage of cells forming clusters: Chondrocyte clustering was occasionally observed in grade-0 (Fig.1(c)), and appeared confined to the superfical zone with only a few cells/cluster. However clustering was routinely observed in grade-1 cartilage (Fig.4(b)). In both grades, the number of clusters was higher in the superficial zone compared to the deep zone (Fig.4(a,b);$P<0.001$;$P<0.05$ respectively). Although the average number of clusters was ~50% greater in the superficial zone of grade-1 compared to grade-0, this was not significant ($P=0.24$). In grade-0 cartilage, the average number of cells/cluster (3.6±0.4) was the same in all zones (Fig.4(c);$P>0.05$). Comparing the superficial zone between grade-0 and grade-1, there was an increase to 9.8±1.7 cells/cluster (Fig.4(d); $P=0.0002$), and the % of superficial zone chondrocytes forming clusters (15.6±3.0% to 61±10.5%;Fig.4(e,f); $P<0.001$). However, although 25% of the mid-zone chondrocytes formed clusters in grade-1 (Fig.4(f)) compared to grade-0 cartilage (~8%; Fig.4(e)), this was not significant. In the deep zone, the number of chondrocytes forming clusters was negligible in both grades (Fig.4(e,f)). When comparing all zones, there was also no significant difference in the average number of clusters (Fig.4(b)), but there was for the average number of cells/cluster (Fig.4(d);$P=0.0001$), and the % of chondrocytes forming clusters (Fig.4(f);$P=0.0013$). This suggests that although the number of clusters was not different between the cartilage grades, more chondrocytes were involved in cluster formation.

(b) Volume of clusters and average volume of chondrocytes within clusters: Average chondrocyte volume in a cluster in grade-0 cartilage was ~5000μm^3 and similar in all zones (Fig.4(g)). However

only in the superficial zone of grade-1 did volume increase significantly, reaching >15,000μm^3 (Fig.4(h);P<0.001) with no significant change in the mid- or deep zone. The average volume of single cells in superficial zone clusters of grade-1 cartilage was ~21% greater compared to those in grade-0 cartilage (Fig.4(j);P=0.04). Although the data for the volume of clusters and volume of individual cells in clusters in the mid- and deep zone of both cartilage grades referred to a relatively small number of clusters, there were no significant differences between zones. While the volume of individual superficial zone chondrocytes in clusters increased with cartilage degeneration, when the average volume of chondrocytes in clusters in all zones were compared, there was no significant difference between grades (Fig.4(i,j)). Furthermore, while the number of clusters did not change, there was a marked increase in the number of cells/cluster, suggesting proliferation was the mechanism for increased cluster size, rather than chondrocyte swelling.

Fine chondrocyte morphology.

(a) Percentage of abnormal chondrocytes: Chondrocytes were categorised into five groups based on the length (L) of cytoplasmic processes: (L0 no processes present, L1<5μm, 5<L2≤10μm, 10<L3≤15μm and L4>15μm). In grade-0 cartilage overall, 17±1.8% chondrocytes exhibited cytoplasmic processes, whereas there were more abnormal chondrocytes in the mid-zone compared to the deep zone (Fig.5(a);P<0.01). In grade-1 cartilage, a significantly higher percentage of chondrocytes had processes compared to grade-0 mainly due to changes in the superficial zone (Fig.5(b);27±3.0%;P=0.0087). A zone-wise analysis of chondrocyte morphology revealed that in the superficial zone of grade-1 cartilage, a higher percentage (36±8%) of chondrocytes had processes compared to the superficial zone of grade-0 cartilage (Fig.5(b);16±2.6%;P=0.0037). Similarly in the mid- and deep zones of grade-1 cartilage, the percentage of chondrocytes with cytoplasmic processes appeared higher (by ~21% and 50% respectively) than those in grade-0 cartilage but not to the significance level.

(b) Average number of cytoplasmic processes/cell: In grade-0 cartilage, the average number of processes/cell (~1.5) was not significantly different in the three zones (Fig.5(c)). In contrast, in

grade-1 cartilage this was significantly higher only in the superficial zone with no significant change in the mid- and deep zones (Fig.5(d);P<0.01). When the zones of grade-0 and grade-1 cartilage were compared, the number of processes/cell was significantly higher only in the superficial zone in grade-1 compared to grade-0 cartilage (Fig.5(d);P=0.02).

(c) Length of cytoplasmic processes: In grade-0 cartilage, cytoplasmic processes in the superficial and mid-zones were ~4.5µm, and significantly greater than those in the deep zone (~2.7µm Fig.5(e);P<0.001 for both). However, in grade-1 cartilage, the average length in the superficial zone (~14µm) was significantly greater than those in mid-zone (~5µm) and deep zone (~4µm) (Fig.5(f); P<0.01 for both). A comparison of average length of cytoplasmic processes in various zones of grade-0 and grade-1 cartilage, revealed significantly longer processes in superficial zone and deep zone of grade-1 compared to grade-0 cartilage (Fig.5(f);P<0.0001;P=0.03 for superficial and deep zones respectively). The percentage of chondrocytes with processes, the number of processes per cell and the average length of processes were all significantly higher in the superficial zone of grade-1 compared to grade-0 cartilage. This suggests that chondrocytes within the superficial zone were more likely to develop processes during cartilage degeneration.

(d) Percentage of chondrocytes with processes of various length categories: The length of cytoplasmic processes ranged from 2-93µm. In order to make comparisons between zones and cartilage grades, the lengths of processes were categorised into 4 groups and the percentage of cells having processes of a specific length category determined. In grade-0 cartilage, for all zones throughout the cartilage, a significantly higher percentage of chondrocytes had L1 processes compared to the other categories (Fig.6(a);P<0.001 for overall data). In grade-1 cartilage, no differences existed between chondrocytes having cytoplasmic processes in L1-L4 categories (overall data; Fig.6(b)). There was no difference between the percentage of chondrocytes having L1 processes in grade-0 and grade-1 cartilage. However, significantly higher percentages of chondrocytes had cytoplasmic processes with L2 and L3 categories in grade-1 as compared to grade-0 cartilage (Fig. 6(b);P<0.05 for both).

Superficial Zone: In grade-0 cartilage, 11±1.2% chondrocytes exhibited L1 processes, which was significantly higher than L2 (5±1% cells) and L3 (1±0.3%) (Fig.6(a);$P<0.01$;$P<0.001$ respectively) and no cells had L4 processes. In contrast, in the superficial zone of grade-1 cartilage, ~12% of the chondrocytes had processes within all length categories compared to grade-0 cartilage, with no significant difference between percentages of chondrocytes in each length category (Fig.6(b);$P>0.05$). When the percentage of superficial zone chondrocytes with processes of various length categories were compared between grade-0 and grade-1, no difference existed with the L1 category, whereas a significantly higher percentage of chondrocytes had processes in L2, L3 and L4 (Fig. 6(b);$P=0.04$;$P=0.03$;$P=0.04$ respectively). Therefore, the percentage of chondrocytes having processes with L2-L4 categories increased in the superficial zone of grade-1 compared to grade-0 cartilage (Fig.6(b)).

Mid Zone: In grade-0 and grade-1 cartilage, the length of processes ranged from L1-L3 with no processes in L4. In both grade-0 and grade-1, a significantly higher percentage of chondrocytes had processes in the L1 category compared to L2 and L3 (Fig.6(a,b);$P<0.01$). When the mid-zone of grade-0 and grade-1 cartilage was compared, no significant difference existed between percentages of cells with processes in L1-L3 length categories. These results suggested that no difference existed between the percentages of chondrocytes with cytoplasmic processes of various lengths in the mid-zone of grade-1 compared to grade-0 cartilage.

Deep Zone: In grade-0 cartilage, only L1 processes were observed. In grade-1, chondrocytes with L1 and L2 were present whereas processes in L3 and L4 categories were absent. In grade-1 cartilage, a significantly higher percentage of chondrocytes had processes in the L1 category compared to L2 (Fig.6(b);$P<0.001$). When the deep zone of grade-0 and grade-1 cartilage was compared, there was no significant difference between the percentages of chondrocytes in the L1 category ($P>0.05$). However, a significantly higher percentage of chondrocytes had processes with L2 category in grade-1 compared to grade-0 cartilage (Fig.6(b);$P=0.0019$). Throughout the cartilage, there existed no difference regarding the presence of L1 processes but a significantly

higher percentage of chondrocytes had processes of L2 and L3 categories in grade-1 compared to grade-0 cartilage (Fig.6(b);*P*=0.0078;*P*=0.039 respectively). Thus, with cartilage degeneration, the percentage of chondrocytes with abnormal morphology, with the number of processes/cell and the average length of cytoplasmic processes increased, and these changes were most pronounced in the superficial zone. When L0 chondrocytes (i.e. those with 'normal' morphology - no cytoplasmic processes) in all zones were compared, overall there was a significant decrease (*P*=0.015) between grade-0 and grade-1 cartilage (Fig. 6(a,b)).

DISCUSSION

Confocal laser scanning microscopy and quantitative imaging identified features of *in situ* chondrocytes in normal (grade-0, non-degenerate) and grade-1 (mildly-degenerate) human femoral head articular cartilage. While some classical aspects of chondrocytes previously reported using standard histological methods were clearly evident (e.g. clustering), the methods used here provided quantifyable data which revealed marked changes to chondrocyte clustering and fine cell morphology between grade-0 and grade-1 cartilage. This allowed a deeper insight into the micro-anatomical properties of normal human cartilage and some of the changes evident with cartilage degeneration than have been obtained to date.

Accurate cartilage grading was essential to ensure that grade-0 and grade-1 cartilage were clearly and reproducibly defined. In addition to the standard criteria (Pritzker et al. 2006), confocal laser scanning microscope imaging of the surface was invaluable as grade-0 cartilage appeared 'smooth' whereas grade-1 cartilage was uneven, allowing discrimination between these grades (Fig.1(c,d)). Careful cartilage grading permitted areas of grade-0 and grade-1 tissue to be studied because of the focal nature of osteoarthritis (e.g. in femoral condyle (Rolauffs et al. 2010; Squires et al. 2003) or tibial plateau; (Squires et al. 2003). In the superficial zone of grade-0 cartilage, chondrocyte clusters were occasionally observed (Figs. 3,4) and this has also been reported in relatively non-degenerate (grade 0-1) cartilage obtained from other joints e.g. distal femur (condyles, patellofemoral groove) and proximal tibia (Rolauffs et al. 2010). However in grade-1 cartilage, clustering increased with the average number of clusters throughout the cartilage, the average number of cells/cluster and the % of cells forming clusters particularly in the superficial zone, increasing significantly (Fig. 4(a-f)). The total volume of clusters and the number of chondrocytes/cluster, suggested that the increase in cluster size was due to chondrocyte proliferation rather than swelling/hypertrophy, as there was only a small increase in superficial zone chondrocyte size (~20%) whereas the volume of clusters increased by >3-fold (Fig. 4(g-h)). This supports previous studies indicating that in human osteoarthritis, cartilage cell proliferation was the

principal mechanism for cluster formation (Lotz et al. 2010). The nature of the peri-cellular matrix (lacuna) surrounding chondrocyte clusters is of interest and could be observed in some confocal images by adjusting the brightness and contrast. Preliminary studies suggested that the lacuna encapsulated the whole cell cluster and that individual lacunae appeared to merge into one large 'bag' surrounding the cell cluster (A. Karim, unpublished).

The majority of chondrocytes within femoral head cartilage were morphologically 'normal' (approximately 80%), however there was a significant decrease from grade-0 and grade-1 (Fig. 6a,b). Despite this, confocal laser scanning microscope imaging of fluorescently-labelled chondrocytes revealed that 15-25% exhibited at least one cytoplasmic process of ~5μm in length (Fig. 5(a)). These processes were unlikely to be due to cutting damage during sampling because abnormal cell morphology was also observed in axial views (Fig.2) where cells were visualised distant from any cut edge. With degeneration to grade-1, marked changes to chondrocyte morphology occurred and there were increases in the percentage of chondrocytes with processes, and the length of processes, particularly for cells in the superficial zone (Fig.5). We should note that the present results relate only to small areas of the cartilage available and it might be premature to assume that the changes reported here are uniform over the whole cartilage surface of the femoral head. Although we compared cartilage from four different regions of the femoral head (parafoveal anterior, parafoveal posterior, parafoveal superior and parafoveal inferior) and found no obvious difference regarding percentage of cells with cytoplasmic processes and the length of these processes, it is quite likely that there on a microscopic scale, there is marked heterogeneity in both chondrocyte morphology and extracellular matrix composition.

At present, we do not have a clear explanation to account for the development of these cytoplasmic processes. They may form 'passively' e.g. from loss/damage to the surrounding pericellular matrix perhaps related to the older donors we studied and aged cartilage which is known to be associated with a reduced size/content of matrix proteoglycans (Dudhia, 2005). However, a previous study on tibial plateau grade-0 cartilage obtained from total knee replacement

operations albeit from a relatively small number of patients (21) and age range (49-86 years), did not find a relationship between the % of normal chondrocytes and patient age (Murray et al., 2010). Disruption to pericellular collagen type VI may also be involved (Guilak et al., 2006; Murray et al. 2010) as its depletion around chondrocytes could provide a weak area into which process(es) could develop. For example, chondrocytes cultured in soft, as opposed to stiff, agarose gels produce cytoplasmic processes with similar structures to those described in the present study (Karim & Hall, 2017). Alternatively, the development of processes could result from mechanically-injured chondrocytes leading to an 'active' metabolic response resulting in the release of cytokines/degradative enzymes and breakdown of the pericellular matrix. It is possible that both 'active' and 'passive' responses are responsible. It is notable that similar chondrocyte cytoplasmic processes of chondrocytes develop in mechanically (scalpel)-injured bovine articular cartilage, but only when fetal calf serum is present (Karim & Hall, 2016). It is possible that the penetration of proliferative factors (e.g. fibroblast growth factor) from the synovial fluid (Quintavalla et al. 2005; Karim & Hall, 2016) through a weakened matrix could actively initiate changes in chondrocyte morphology.

There is a close relationship between chondrocyte shape and matrix metabolism (Von der Mark et al. 1977; Cancedda et al. 1995). Chondrocyte de-differentiation to a fibroblastic-like phenotype which is characterised by cytoplasmic processes, reduces synthesis/release of cartilage-specific components e.g. collagen type II, aggrecan, and increases collagen type I and small proteoglycan production (Stokes et al. 2002). Changes in chondrocyte shape also stimulate levels of agents implicated in extracellular matrix breakdown (Page-McCaw et al. 2007) leading to a localised matrix loss (Hollander et al. 1995) potentially further increasing the development of cytoplasmic processes. A central role for transforming growth factor β1-induced signalling in human osteoarthritis has been reported, which may promote a fibroblastic phenotype (Plaas et al. 2011). The presence of abnormal and/or clustered chondrocytes, with compromised matrix metabolism in otherwise non-degenerate (grade-0) cartilage, could indicate an early weakening in the association

between chondrocytes and surrounding peri-cellular matrix, and increase vulnerability to mechanical loading (Alexopoulos et al. 2005). This could raise the possibility of chondrocyte injury/death increasing the risk of cartilage degeneration (Hashimoto et al. 1998; Del Carlo & Loeser, 2008). It would be of particular interest to determine the influence of the morphological changes reported here on the cytoskeletal structure of *in situ* chondrocytes, matrix metabolism and the structure/composition of the pericellular and bulk extracellular matrix.

These results suggested that even in apparently normal, non-degenerate cartilage, the spatial organisation (clustering) and morphology (cytoplasmic processes) of chondrocytes is altered from that which is classically described in the literature. It is known that a change in chondrocyte morphology indicates the loss of phenotype associated with the maintenance of a cartilage-specific and resilient extracellular matrix capable of withstanding mechanical load (Aigner et al, 2007). The presence in otherwise normal cartilage of a relatively small population of chondrocytes as clusters and/or with morphological abnormalities could reflect local physico-chemical conditions, cartilage age or pericellular matrix integrity. The present results which demonstrated increased chondrocyte clustering and morphological abnormalities with cartilage degeneration, identified aberrant chondrocytes which are potentially producing a defective and weakened extracellular matrix.

Acknowledgements.

This study was funded by the University of Health Sciences, Lahore and Higher Education Commission, Pakistan, and the College of Medicine and Veterinary Medicine, University of Edinburgh. We thank Dr A. Kubasik-Thayil for expert assistance with the confocal scanning laser microscope.

Author's contributions.

Conception and design: AK, AA, ACH.

Analysis, statistical evaluation and interpretation of data: AK, AA, ACH.

Drafting of the manuscript: AK, ACH.

Critical revision of the article for important intellectual content: AK, AA, ACH.

Final approval of the manuscript: AK, AA, ACH.

Conflict of Interest. The authors do not have any Conflicts of Interest to declare in relation to the work presented here.

REFERENCES

Aigner, T, Soder S, Gebhard PM, et al. (2007) Mechanisms of disease: role of chondrocytes in the pathogenesis of osteoarthritis – structure, chaos and senescence. *Nat Clin Pract Rheumatol* **3**(3), 391-399.

Alexopoulos LG, Setton LA, Guilak F (2005) The biomechanical role of the pericellular matrix in articular cartilage. *Acta Biomat* **1**, 317-325.

Amin AK, Bush PG, Huntley JS, et al. (2008) Osmolarity influences chondrocyte death in wounded articular cartilage. *J Bone Joint Surg* **90**, 1531-1542.

Aydelotte MB, Kuettner KE (1988) Difference between sub-population of cultured bovine articular chondrocytes. I. Morphology and cartilage matrix production. *Conn Tiss Res* **18**[3], 205-222.

Benya PD, Shaffer JD (1982) Dedifferentiated chondrocytes re-express the differentiated collagen phenotype when cultured in agarose gels. *Cell* **30**, 215-224.

Blaine EJ (2009) Involvement of the cytoskeletal elements in articular cartilage homeostasis and pathology. *Int J Exp Pathol* **90**, 1-15.

Buckwalter JA, Mankin HJ (1997) Articular cartilage. Part II. Degeneration and osteoarthrosis, repair regeneration and transplantation. *J Bone Joint Surg* **79**[4], 612-632.

Bush PG, Hall AC (2001) The osmotic sensitivity of isolated and in situ bovine articular chondrocytes. *J Orthop Res* **19**[5], 768-778.

Bush PG, Hall AC (2003) The volume and morphology of chondrocytes within non-degenerate and degenerate human articular cartilage. *Osteoarthritis Cartilage* **11**[4], 242-251.

Cancedda R, Descalzi-Cancedda F, Castagnola P (1995) Chondrocyte differentiation. *Int Rev Cytol* **59**, 265-358.

Chen SS, Falcovitz YH, Schneiderman R, et al. (2001) Depth-dependent compressive properties of normal aged human femoral head articular cartilage: relationship to fixed charge density. *Osteoarthritis Cartilage* **9**[6], 561-569.

Del Carlo M Jr, Loeser RF (2008) Cell death in osteoarthritis. *Curr Rheumatol Rep* **10**[1], 37-42.

Dudhia J (2005) Aggrecan, aging and assembly in articular cartilage. *Cell Mol Life Sci* **62**, 2241-2256.

Dowthwaite GP, Bishop JC, Redman SN, Khan IM, Rooney P, Evans DJ, Haughton L, Bayram Z., Boyer S, Thomson B, Wolfe MS, Archer CW (2004). The surface of articular cartilage contains a progenitor cell population. *J Cell Sci* **117**:889-97.

Grodzinsky AJ, Levenston ME, Jin M, et al. (2000) Cartilage tissue remodelling in response to mechanical forces. *Ann Rev Biomed Eng* **2**, 691-713.

Guilak F, Alexopoulos LG, Upton ML, et al. (2006) The pericellular matrix as a transducer of biomechanical and biochemical signals in articular cartilage. *Ann NY Acad Sci* **1068**, 498-512.

Hashimoto S, Ochs RJ, Komiya S, Lotz M (1998) Linkage of chondrocyte apoptosis and cartilage degeneration in human osteoarthritis. *Arthritis Rheum* **41**, 1632-1638.

Hembree WC, Ward BD, Furman BD, et al. (2007) Viability and apoptosis of human chondrocytes in osteochondral fragements following joint trauma. *J Bone Joint Surg* **89**[10], 1388-1395.

Hollander AP, Pidoux I, Reiner A, et al. (1995) Damage to type II collagen in aging and osteoarthritis starts at the articular surface, originates around chondrocytes, and extends into the cartilage with progressive degeneration. *J Clin Invest* **96**, 2859-2869.

Holloway I, Kayser M, Lee DA, et al. (2004) Increased presence of cells with multiple elongated processes in osteoarthritic femoral head cartilage. *Osteoarthritis Cartilage* **12**[1], 17-24.

Huntley JS, Simpson AH, Hall AC (2005) Use of non-degenerate human osteochondral tissue and confocal laser scanning microscopy for the study of chondrocyte death at cartilage surgery. *Europ Cells Mat* **9**, 13-22.

Hunziker EB (1992) Articular cartilage structure in humans and experimental animals. In Articular Cartilage and Osteoarthritis. K.E. Kuettner, R. Schleyerbach, J.G. Peyron & V.C. Hascall. (Eds.) New York, Raven Press, pp. 183-199.

Karim A, Hall AC (2016) Hyperosmolarity normalizes serum-induced changes to chondrocyte properties in a model of cartilage injury. *Europ Cells Mat* **31**, 205-220.

Karim A, Hall AC **(**2017) Chondrocyte morphology in stiff and soft agarose gels and the influence of fetal calf serum. *J Cell Phys* **232**(5), 1041-1052.

Kouri JB, Arguello C, Luna J, et al. (1998) Use of microscopical techniques in the study of human chondrocytes from osteoarthritic cartilage: An overview. *Micros Research Tech* **40**, 22-36.

Lotz MK, Otsuki S, Grogan SP, et al. (2010) Cartilage cell clusters. *Arthritis Rheum* **62**[8], 2206-2218.

Mallein-Gerin F, Garrone R, van der Rest M (1991) Proteoglycan and collagen synthesis are correlated with actin organisation in dedifferentiating chondrocytes. *Eur J Cell Biol* **56**, 364-373.

McGlashen SR, Cluett EC, Jensen CG, et al. (2008) Primary cilia in osteoarthritic chondrocytes: from chondrons to clusters. *Develop Dyn* **237**[8], 2013-2020.

Murray DH, Bush PG, Brenkel IJ, et al. **(**2010) Abnormal human chondrocyte morphology is related to increased levels of cell-associated IL-1β and disruption to pericellular collagen type VI. *J Orthop Res* **28**[11], 1507-1514.

Page-McCaw A, Ewald AJ, Werb Z (2007) Matrix metalloproteinases and the regulation of tissue remodelling. *Nature Rev Mol Cell Biol* **8**, 221-233.

Paterson SI, Amin AK, Hall AC (2015) Airflow accelerates bovine and human articular cartilage drying and chondrocyte death. *Osteoarthritis Cartilage* **23**, 257-265.

Plaas A, Velasco J, Gorski DJ, et al. (2011) The relationship between fibrogenic TGFβ1 signalling in the joint and cartilage degradation in post-injury osteoarthritis. *Osteoarthritis Cartilage* **19**, 1081-1090.

Poole CA, Matsuoka A, Schofield JR (1991) Chondrocyte from articular cartilage. III Morphologic changes in the cellular microenvironment of chondrons isolated from osteoarthritic cartilage. *Arthritis Rheum* **34**[1], 22-35.

Pritzker KPH, Gay S, Jimenez SA, et al. (2006) Osteoarthritis cartilage histopathology: grading and staging. *Osteoarthritis Cartilage* **13**, 13-29.

Quintavalla J, Kumar C, Daouti S, et al. (2005) Chondrocyte cluster formation in agarose cultures as a functional assay to identify genes expressed in osteoarthritis. *J Cell Physiol* **204**, 560-566.

Rolauffs B, Williams JM, Aurich M, et al. (2010) Proliferative re-modelling of the spatial organisation of human superficial chondrocytes distant to focal early osteoarthritis (OA). *Arthritis Rheum* **62**[2], 489-498.

Rothwell AG, Bentley G (1973) Chondrocyte multiplication in osteoarthritic articular cartilage. *J Bone Joint Surg* **55**, 588–594.

Rottmar M, Mhanna R, Guimond-Lischer S, et al. (2014) Interference with the contractile machinery of the fibroblastic chondrocyte cytoskeleton induces re-expression of the cartilage phenotype through involvement of PI3K, PKC and MAPKs. *Exp Cell Res* **320**[2], 175-187.

Schumacher BL, Su JL, Lindley KM, et al. (2002) Horizontally oriented clusters of multiple chondrons in the superficial zone of ankle, but not knee articular cartilage. *Anat Rec* **266**, 241-248.

Shibakawa A, Aoki H, Masuko-Hongo K, et al. (2003) Presence of pannus-like tissue on osteoarthritic cartilage and its histological character. *Osteoarthritis Cartilage* **11**, 133-140.

Simpkin, V, Murray, DH, Hall AP, et al. (2007) Bicarbonate-dependent pH_i regulation by chondrocytes within the superficial zone of bovine articular cartilage. *J Cell Physiol* **212**[3], 600-609.

Squires GR, Okouneff S, Ionescu M, et al. (2003) The pathobiology of focal development in aging human articular cartilage and molecular matrix changes characteristic of osteoarthritis. *Arthritis Rheum* **48**[5], 1261-1270.

Stokes DG, Liu G, Dharmavaram R, et al. (2001) Regulation of type-II collagen gene expression during human chondrocyte de-differentiation and recovery of chondrocyte-specific phenotype in culture involves Sry-type high-mobility-group box (SOX) transcription factors. *Biochem J* **360**[2], 461-470.

Stokes DG, Liu G, Coimbra IB, et al. (2002) Assessment of the gene expression profile of differentiated and dedifferentiated human fetal chondrocytes by microarray analysis. *Arthritis Rheum* **46**[2], 404-419.

Tesche F, Miosge N (2005). New aspects of the pathogenesis of osteoarthritis: the role of fibroblast-like chondrocytes in late stages of the disease. *Histol Histopathol* **20**, 329-337.

Vanderploeg EJ, Wilson CG, Levenston ME (2008) Articular chondrocytes derived from distinct tissue zones differentially respond to in vitro oscillatory tensile loading. *Osteoarthritis Cartilage* **16**, 1228-1236.

Von der Mark JK, Gauss V, von der Mark H, et al. (1977) Relationship between cell shape and type of collagen synthesised as chondrocytes lose their cartilage phenotype in culture. *Nature* **267**, 531-532.

Wong M, Wuethrich P, Eggli P, et al. (1996) Zone-specific cell biosynthetic activity in mature bovine articular cartilage: a new method using confocal microscopic stereology and quantitative autoradiography. *J Orthop Res* **14**[3], 424-432.

Woods A, Wang G, Beier F (2007) Regulation of chondrocyte differentiation by the actin cytoskeleton and adhesive interactions. *J Cell Physiol* **213**, 1-8.

FIGURE LEGENDS

Figure 1: Macroscopic and microscopic overview of grade-0 and grade-1 human femoral articular cartilage. The upper two panels show examples of the macroscopic appearance of human femoral heads obtained from (a) a male patient (64yrs) and (b) a female patient (85yrs) with cartilage graded at the solid arrows as grade-0 and grade-1 respectively. The broken arrows indicate the fovea. Macroscopic grading of cartilage was initially performed using Osteoarthritis Research Society International criteria, followed by a microscopic grading which was determined by studying the cartilage surface of the explants to be imaged (see Materials and Methods). The lower two panels show representative confocal scanning laser microscopy low power (x10) images of 5-chloromethylfluorescein diacetate and propidium iodide labelled chondrocytes viewed in the coronal plane in (c) grade-0 and (d) grade-1 cartilage. The approximate thicknesses of the zones (SZ = superficial zone; MZ = mid-zone; DZ = deep zone) are shown. Grade-0 cartilage showed a smooth regular surface with minor morphological changes to chondrocytes, whereas grade-1 displayed obvious surface discontinuity and erosions with chondrocyte clustering. Cytoplasmic processes of chondrocytes could not be visualised at this magnification. Solid arrows indicate smooth and rough surfaces of grade-0 and grade-1 cartilage respectively, double headed arrows indicate areas of hypo-cellularity and broken arrows indicate examples of chondrocyte clusters present in grade-1 cartilage. (Scale bar for all panels and inset image =100µm and 50µm respectively).

Figure 2: Low and high power axial confocal laser scanning microscope reconstructed images of chondrocytes within grade-0 and grade-1 human femoral head articular cartilage. Representative examples of confocal laser scanning microscope images at low magnification (x10) 5-chloromethylfluorescein diacetate and propidium iodide - labelled chondrocytes (live and dead cells respectively) in human (a) grade-0 and (b) grade-1 cartilage explants. At low magnification,

chondrocyte morphology and distribution in grade-0 cartilage appeared relatively normal however in mildly-degenerate (grade-1) samples, evidence of chondrocyte clustering (solid arrow) and areas of hypo-cellularity were present (double-headed arrows). (Scale bar for both panels and the inset =100µm and 50µm respectively). At high magnification (panel (c)) (x40), the majority of chondrocytes in grade-0 cartilage demonstrated normal morphology, however some cells with short, often curled, cytoplasmic processes were present (solid arrows) with infrequent clustering of chondrocytes (≥3 cells; broken arrow). In grade-1 cartilage (d), many cells possessed cytoplasmic processes of varying length (solid arrows) and number, and there was extensive clustering (inset in (b), and broken arrow in (d)). Note that there were no propidium-labelled chondrocytes detected in these images even though this fluorescent indicator was present. (Scale bar for both panels =25µm).

Figure 3: High power coronal confocal laser scanning microscope reconstructed images of chondrocytes within grade-0 and grade-1 human femoral articular cartilage. High power (x40) coronal images of fluorescently-labelled chondrocytes (5-chloromethylfluorescein diacetate and propidium iodide for live and dead cells respectively) were imaged in regions corresponding to the superficial, mid- and deep zones (SZ, MZ, DZ respectively) of grade-0 (a, c, e) and grade-1 (b, d, f) cartilage. Solid arrows show examples of cells with cytoplasmic processes and broken arrows indicate examples of clusters present in various zones of cartilage. (Scale bar for all panels =25µm).

Figure 4: Analysis of chondrocyte clusters in human femoral grade-0 and grade-1 articular cartilage. Histograms show pooled data for (a,b) average number of clusters, (c,d) average number of cells per cluster, (e,f) percentage of cells present in clusters, (g,h) average volume of clusters (μm^3) and (i,j) average volume of individual cells in a cluster (μm^3) in the superficial, mid- and deep zones (SZ, MZ, DZ respectively) of grade-0 and grade-1 explants respectively. Data were from [*N(n)*=11(1398)] for grade-0 and [*N(n)*=5(551)] for grade-1 cartilage explants. In this and subsequent Figures, data are shown as mean ± CI (95%). A hash symbol (#) indicated a significant

difference according to one-way Analysis of Variance followed by Tukey's multiple comparison *post-hoc* test. An asterisk (*) showed a significant difference between grade-0 and grade-1 cartilage explants according to an unpaired Student's t-test. Some important comparisons which were not significantly different, are indicated N/S. The single, double and triple symbols showed the level of significance at $P<0.05$, 0.01 and 0.001 respectively.

Figure 5: Morphological characteristics of chondrocytes in grade-0 and grade-1 human femoral head articular cartilage. Histograms show pooled data regarding (a,b) percentage of cells with cytoplasmic processes, (c,d) number of processes per cell and (e,f) average length of cytoplasmic processes (μm) in the superficial, mid- and deep zones (SZ, MZ, DZ respectively) of grade-0 and grade-1 cartilage respectively. Data (mean ± confidecne intervals (95%)) were from [*N(n)*=11(1398) and 5(551)] for grade-0 and grade-1 cartilage explants respectively. A hash symbol (#) indicated a significant difference according to one-way Analysis of Variance followed by Tukey's multiple comparison *post-hoc* test. An asterisk (*) showed a significant difference between grade-0 and grade-1 cartilage explants according to Student's t-test. The single, double and triple symbols showed the level of significance for $P<0.05$, 0.01 and 0.001 respectively.

Figure 6: Abnormal chondrocyte morphology with cartilage depth and grade. Histograms show pooled data for the percentage of chondrocytes with cytoplasmic processes of various lengths in the superficial, mid- and deep zones (SZ, MZ, DZ respectively) of (a) grade-0 and (b) grade-1 human femoral head articular cartilage respectively. Data (mean ± confidence intervals (95%)) were from [*N(n)*=11(1398) and 5(551)] for grade-0 and grade-1 cartilage explants respectively. A hash symbol (#) indicated a significant difference according to one-way Analysis of Variance followed by Tukey's multiple comparison *post-hoc* test. An asterisk (*) showed a significant

difference between grade-0 and grade-1 cartilage explants according to Student's t-test. The single, double and triple symbols showed the level of significance for $P<0.05$, 0.01 and 0.001 respectively.

Karim et al (2017)
Figure 1.

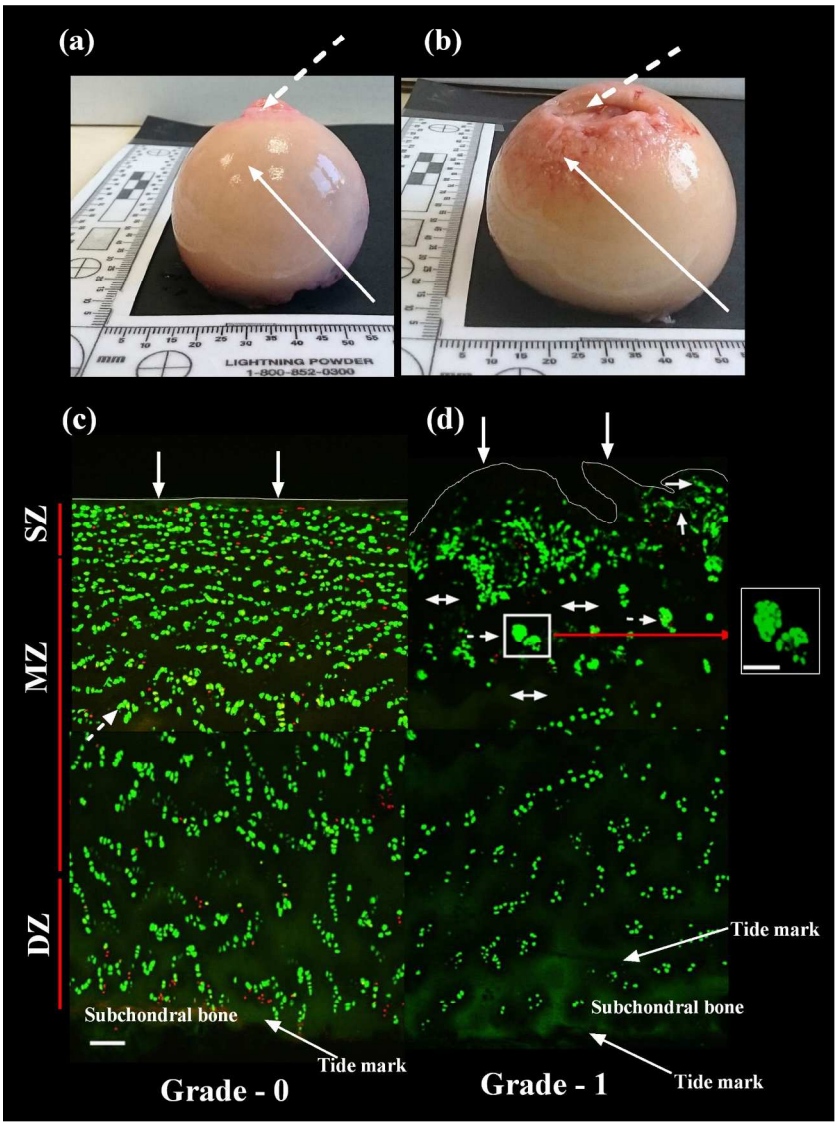

Karim et al (2017) Figure 1

275x397mm (300 x 300 DPI)

Karim et al (2017)
Figure 2

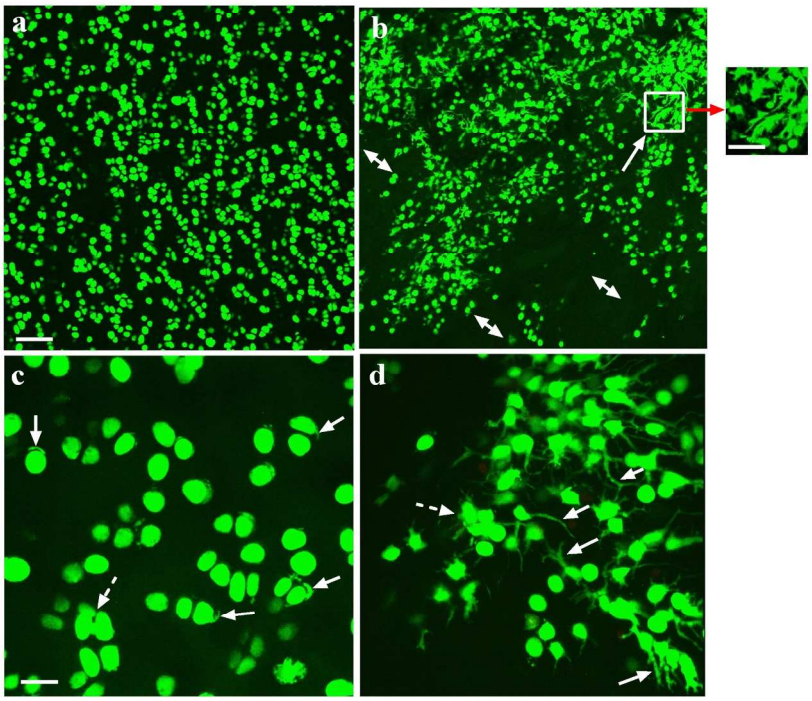

Karim et al (2017) Figure 2

275x397mm (300 x 300 DPI)

Karim et al (2017)
Figure 3

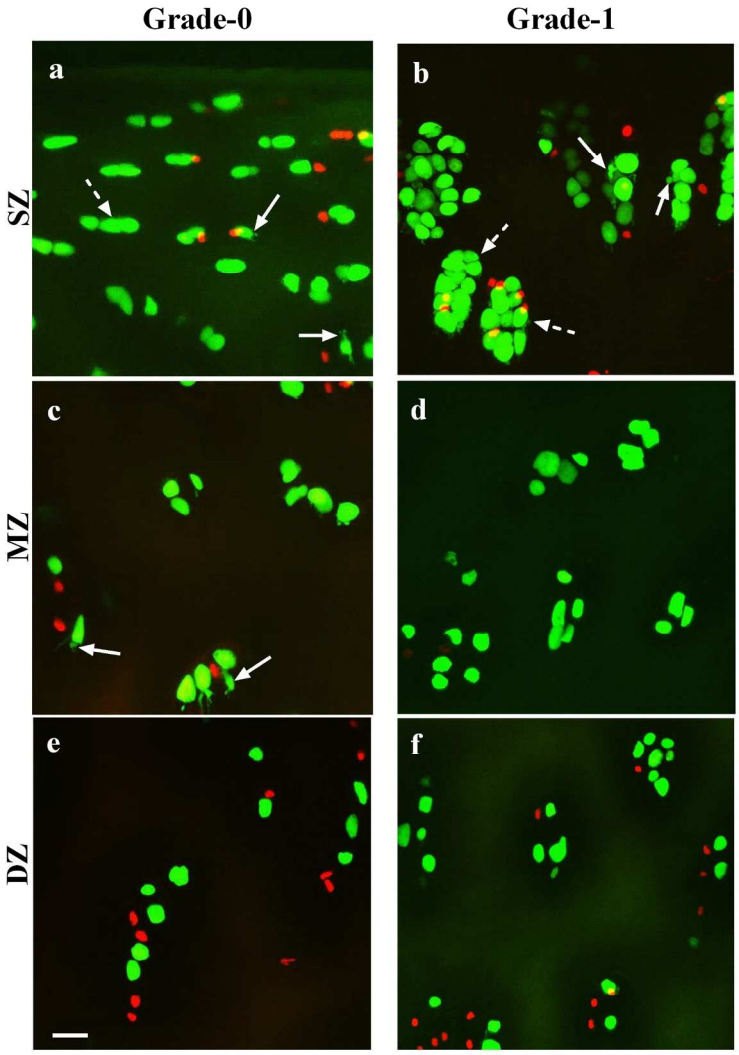

Karim et al (2017) Figure 3

275x397mm (300 x 300 DPI)

Karim et al (2017)
Figure 4

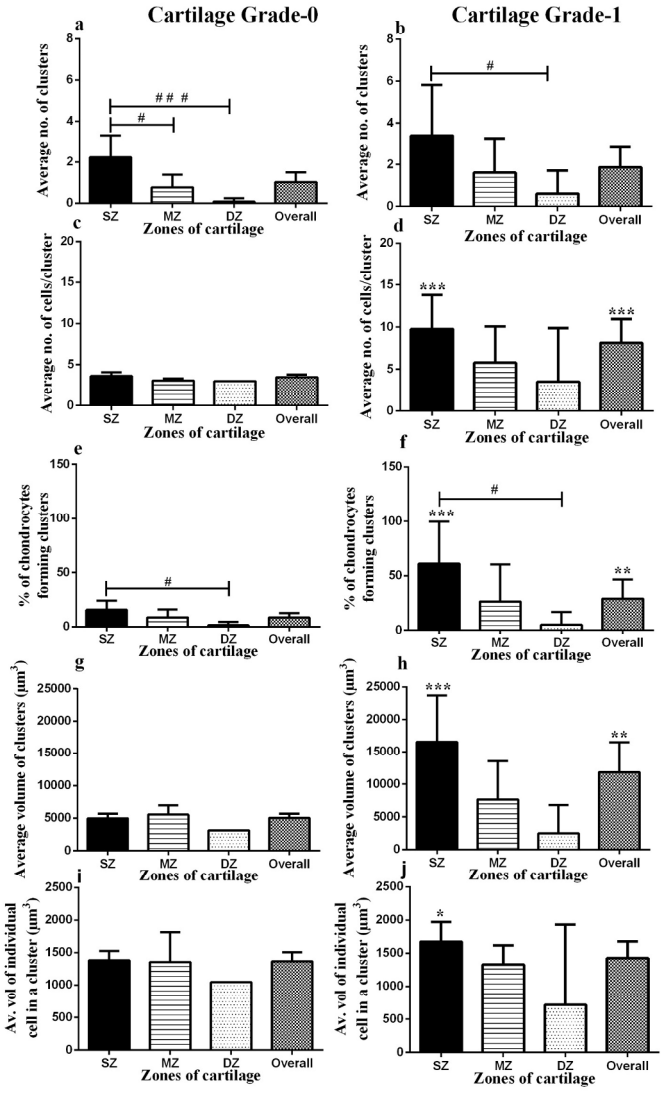

Karim et al (2017) Figure 4

275x397mm (300 x 300 DPI)

Karim et al (2017)
Figure 5

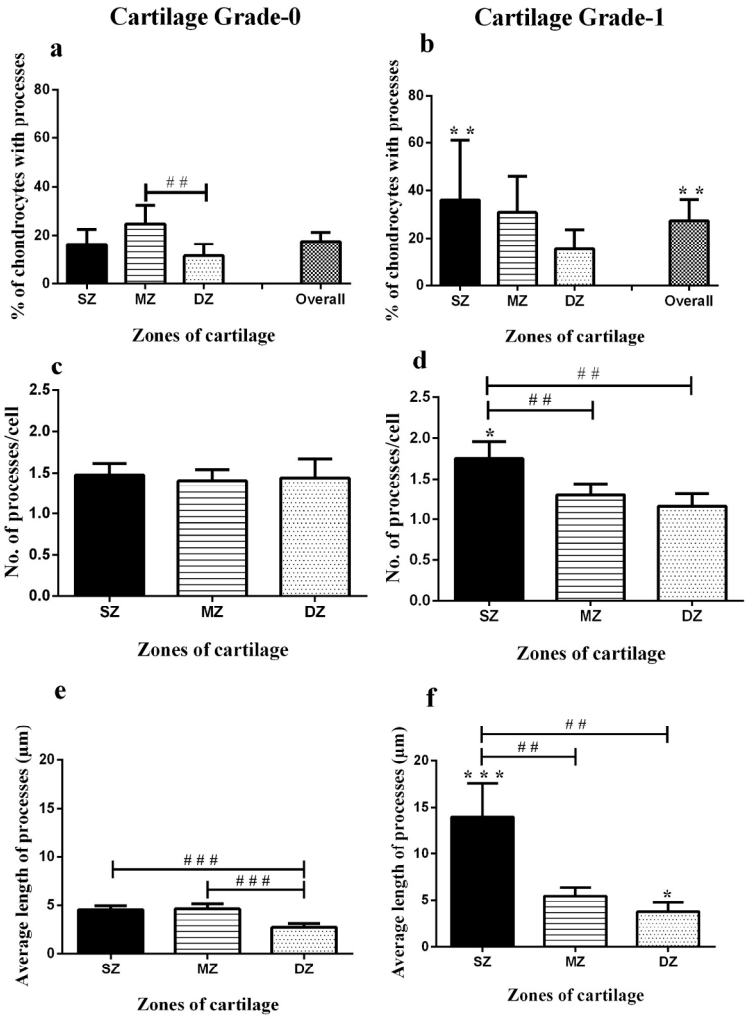

Karim et al (2017) Figure 5

275x397mm (300 x 300 DPI)

Karim et al (2017)
Figure 6.

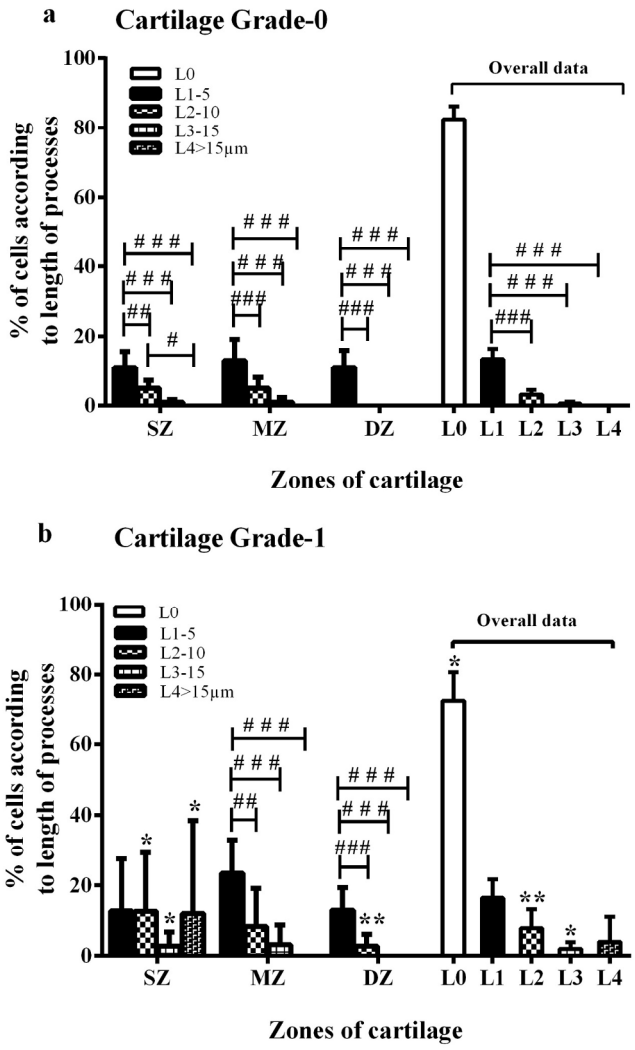

Karim et al (2017) Figure 1

275x397mm (300 x 300 DPI)